RSC Advances

Electrochemical degradation of RB19 dye using low-frequency alternating current: Effect of a square wave

Edris Hoseinzadeh, Abbas Rezaee*

Environmental and Occupational Health Dept., Faculty of Medical Sciences, Tarbiat Modares University, Tehran, Iran; Tel: +98 21 82883575; E-mail: rezaee@modares.ac.ir (A. Rezaee)

ABSTRACT

This study mainly aims to investigate effects of alternating current (AC) on Remazol Brilliant Blue R (RB19) dye removal from aqueous solutions by electrochemical (EC) process. Effects of operating conditions on RB19 removal were investigated; the conditions include AC frequency, Magnitude of a waveform in Vpp (AMPL) accompanied with a constant voltage that is added to an AC source (OFST), supporting electrolyte (type and concentration), and initial dye concentration. Moreover, effects of variation in electrical conductivity, oxidation–reduction potential, and pH on the efficacy of the process were evaluated. Results showed that the highest RB19 removal efficiency with low electrode weight loss was obtained at AMPL and OFST of 8 Vpp and 0.2 V, respectively. Results of our kinetic study showed that the addition of NaCl as a supporting electrolyte has an enhancing effect on the rate constant, possibly because of increase in the concentration of active oxidant species such as Cl_2/OCl^- in the electrolyte. Morphology study on the electrode surface showed that electrodes dissolved

uniformly during the EC process. Loss on ignition (LOI) was determined to be 43.25% by X-ray fluorescence (XRF) analysis. Energy consumption and operating costs for RB19 removal using a square wave AC were evaluated. The result indicated that the use of a square wave AC is a promising wastewater treatment technique.

Keywords: Alternative current, electrochemical, Wastewater, Textile, Energy consumption.

1. Introduction

Over the past 10 years, electrochemical (EC) process has been most widely accepted for the removal of wastewater pollution [1, 2]. EC process subsets, which are used for removing dye from aqueous solutions, include electrocoagulation, EC reduction, EC oxidation, indirect electro-oxidation with powerful oxidants (electro-oxidation with active chlorine, electro-Fenton), and photo-supported EC methods (photoelectro-Fenton, photoelectrocatalysis) [3, 4]. Because of the rather large capital investment and high cost of electricity associated with the development, practical application of EC techniques in water and wastewater treatment had been hindered worldwide. Drinking water and wastewater effluent standards' promotion and establishment of strict environmental legislations resulted in renewed importance and development of EC techniques, especially for the past two decades[2, 5]. Today, because of extensive research, this technology has reached a level of development

that is not only competitive with other technologies in aspect of cost efficient, but also much more efficient and more competitive in terms of cost [2]. In addition, sometimes in case of inorganic or organic pollutants, EC technique is an essential and crucial step in wastewater treatment [6]. Frequently, direct current (DC) is used in EC process for treating dye wastewater at relatively low voltages and relatively high currents[2, 7]. Financial inducements in performing EC process with alternating currents (ACs) are numerous, one of them being the elimination of AC to DC conversion costs. Meanwhile, in DC EC process, a passive film may form on the cathode leading to ineffective current transfer between electrodes[8], as a result of which, the treatment efficiency decreases. This problem is resolved by using AC EC process utilizing cyclic frequencies between the anode and the cathode. Many reports on treatment of synthetic or real wastewater with DC EC process are available[9-12], while only a small number of studies have reported on low-frequency AC EC process with different wave shapes and operating costs based on the required electrical energy and electrodes. On the other hand, chemical dyes or un-natural dyes that are used in different industries such as textile industries, paper, tanning of leather, food processing, plastic, cosmetics, rubber, printing, and dye manufacturing industries are multipart organic molecules, which are used for different substances painting[13, 14]. Chemical dyes should have long-lasting property, so they are resistant against degradation. Dye effluent into the

environment, especially water bodies, which leads to decreased penetration of sunlight reducing its re-oxygenation ability, accounts for a considerable pollutant[10, 15, 16]. Although accurate data on the quantity of dye effluent from a variety of processes in the environment is not available, the discharge of synthetic dyes to the environment even in low quantity has created challenges to environmental scientists. According to available data, there are over 10^5 commercial dyes worldwide; more than 7×10^5 tons of dyes are produced per year, 5%–10% of which is discharged into wastewater or water bodies[17]. Among dye consuming industries, the textile dyeing industry is recognized to be one of the major environmental pollution contributors. Textile dyeing industry also consumes large volumes of clean water. Dye containing aqueous solution treatment and water-reuse can play a noteworthy role in reducing discharge of dye wastewater and providing reusable water for processing. Simply because of their water solubility, reactive azo dyes that have one or more azo groups (R1–N=N–R2) and aromatic rings typically replaced by sulfonate groups are one of the most widely used in textile industry for dyeing cellulosic fibers, silk, wool, nylon, and leather[13]. Reactive dyes set up covalent bonds with hydroxyl or amino groups of the dyed material resulting in good fixation[6]. Remazol Brilliant Blue R or Reactive Blue 19 dye is an anthraquinone-based vinyl sulphone dye, one of the most widely used reactive dyes. As RB19 is stable and steady, and has low biodegradability in the

aquatic environment for a long time[6], (with the half-life being 46 years at pH 7 and at 25°C), it has been used as a model in dye removal studies. Methods with physical or chemical bases such as adsorption, chemical transformation, incineration, electrocoagulation, photocatalysis or ozonation, and biological or enzymatic treatment are the most reported methods for treating dye wastewater. The exact novelty of this work is use low voltage and low frequency alternating current. Additionally, in the present work we used function generator as a supply source. Usage function generator able us to study AC EC as a function of different waveform, different current frequency (commonly the frequency of distribution network is 50 or 60 Hz), and use magnitude of a waveform and an adjustable DC voltage added to the signal output (DC offset), simultaneously. Therefore, in this study, removal of RB19 from aqueous solutions with stainless steel 304 electrodes in a batch using a very low frequency square wave AC was investigated in terms of technical aspects and operating costs. This study finding can introduce new configuration for electrochemical systems, especially AC ECs.

2. Methods

2.1. Materials

Materials used were marketable-grade stainless steel (SS) 304 electrodes as shown in Table 1 (17 cm × 3 cm × 1 mm, total immersed surface area=51 cm^2), distilled

water, RB19 (Alvan Sabet, Iran; refer to Table 2). Na_2SO_4 or NaCl (GR, Qualigens, Mumbai, India) was used as a supporting electrolyte.

2.2. Experimental setup

The experimental setup (Fig. 1) consists of a 500 mL capacity Plexiglas vessel of 0.5 cm in thickness, SS 304 electrodes with 2 cm distance between the two, AFG-2000 function generator (GW INSTEK; 0–10 Vpp, 0.056 A, 50 Ω), and a magnetic stirrer (Shoimiazma, Iran). In case of the function generator, the term peak-to-peak voltage (Vpp) refers to the maximum AC voltage.

2.2. Experimental procedure

All the experiments were performed in a 500 mL capacity Plexiglas vessel in batch mode. Each batch contained 350 mL of RB19 aqueous solution. After each run, samples were analyzed with an UV/Vis spectrophotometer (Perkin-Elmer 550 SE, USA) at its maximum absorption wavelength (λ_{max}=592 nm). Oxidation-reduction potential of each sample was measured with an ORP meter (Eutech, Singapore), temperature and electrical conductivity with HI 98129 (HANA), and pH with HQ40d (Hach). Surface morphology of the electrodes was analyzed with a 13MP, Samsung Galaxy Note 3 cameral, and an elemental analysis of electro-oxidation of RB19 sludge was performed with an X-ray fluorescence (XRF) and scanning electron microscopy (SEM) spectrometer: both instruments located at the Faculty of Science, Tarbiat Modares University, Tehran, Iran.

2.3. Determination of rate constant

In the performed experiments, the removal efficiency of RB19 was investigated in terms of the initial RB19 concentration, the type and amount of electrolyte, and AC frequency, as well as with or without solution stirring; all experimental results obtained for RB19 removal as a function of electro-oxidation time were matched with the pseudo-first order reaction kinetics[18]:

$$\ln(\frac{C}{C_0}) = -k \times t \tag{1}$$

where C is the concentration of RB19 (mg/L) at electro-oxidation time = t, and C_0 the initial concentration of RB19 at time =0 or prior to the EC process; k is the pseudo-first order RB19 removal constant obtained for EC process (min^{-1}). The constant k can be calculated from ploting of $\ln(C/C_0)$ vs. electro-oxidation time (min). The percentage of color removal was calculated using the following equation:

$$\text{RB19 removal (\%)} = \frac{Abs_0 - Abs_t}{Abs_0} \times 100 \tag{2}$$

3. Results and Discussion

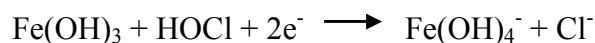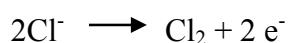### 3.1. Effects of applied voltage' on RB19 removal

RB19 removal efficiency was considerably affected by the applied voltage. Here, the applied voltage consists of an AC component and a DC offset. The peak-to-peak value of the AC signal is adjusted by AMPL (Magnitude of a waveform in Vpp) and the amplitude of the DC offset (a constant voltage that is added to an AC

source) by OFST keys. The highest RB19 removal efficiency with low electrode weight loss or corrosion was observed when AMPL and OFST were set at 8 Vpp and 0.2 V, respectively (Fig. 2). The high RB19 removal efficiency may be due to the amount of OCl⁻ kinds produced under this condition[2, 7]. In succeeding experiments, AMPL=8 Vpp and OFST=0.2 V were applied as the input voltage.

3.2. The role of supporting electrolyte

Two different salts, namely NaCl and Na_2SO_4, were studied as a supporting electrolyte to select one with the higher dye removal efficiency for the subsequent EC tests. With V_{rms} =2.828 or V = 8 Vpp, OFST =0.2 V, and the duty cycle= 95% kept constant, different amounts of the salts were added to the RB19 solution. The efficiency of RB19 removal was determined for various RB19 concentration (mg/L), AC frequency (Hz), and electro-oxidation time (min) at two modes: one with and the other without solution stirring. Use of NaCl as an electrolyte resulted in considerable RB19 removal even without solution stirring. When stirred, both NaCl and Na_2SO_4 were useful in RB19 removal, but NaCl had a higher removal efficiency. The minimum amount of NaCl used for RB19 removal was lower than that of Na_2SO_4 in case of the stirring solution mode. The RB19 removal percentage was 95.12% ± 1.4% at the maximum treatment time of 60 to 120 min in case of NaCl, while the obtained mean removal percentage for Na_2SO_4 was 45.56% ± 20.7% at 180 to 210 min treatment time. The increased rate of RB19 removal

8

observed with the use of NaCl instead of Na_2SO_4 may be due to enhancement of

chlorine/hypochlorite production under galvanostatic conditions[19]. Concurrent

creation of O_2 and Cl_2 occurs when the discharge potential of Cl_2 is near to that of

O_2, in which case, the rate of Cl_2 production is reduced. There is no dye removal in

case of Na_2SO_4 without stirring. In the non-stirring mode, a mean RB19 removal

efficiency of $74.3\% \pm 20.04\%$ (30.08% to 99.47%) was obtained for 0.5 to 5 g/L of

NaCl used, and the minimum time to achieve dye removal was 78.9 ± 15.13 min.

As NaCl concentration increases, the discharge potential of Cl_2 decreases

according to the Nernst equation, resulting in more current consuming. In this case,

Cl_2 and hypochlorite generation increases as well. Therefore, the higher RB19

removal efficiency is obtained. Presence of more NaCl enhances the generation

rate of mononuclear and poly-nuclear $Fe(OH)_3$ by the sequence of reactions shown

in the following equations and improves RB19 removal:

$$2Cl^- \longrightarrow Cl_2 + 2\ e^-$$

$$Cl_2 + H2O \longrightarrow HOCl + H+ + Cl^-$$

$$Fe(OH)_3 + HOCl + 2e^- \longrightarrow Fe(OH)_4^- + Cl^-$$

The amount of NaCl does not show significant relations with RB19 concentration,

AC frequency, and weight loss of electrodes ($P> 0.05$) with their Pearson's

correlation being -0.075, 0.043, and -0.236, respectively. The correlation indicates

a negative linear relation between NaCl amount in the solution and RB19

concentration, and between NaCl amount and weight loss of electrodes; however, there is a linear relation between NaCl amount in the solution and AC frequency.

Stirring provides a homogeneous dye solution in the EC reactor resulting in efficient RB19 removal, but stirring at high speeds (greater than 400 rpm) diminishes potential for flock creation yielding a lower efficiency[20]. Without the stirring mode no homogeneous dye solution is obtained in the EC reactor, so the formed flocks sediment between electrodes[21]; therefore, cell resistance at low stirring speed is desirable. Of course, the produced H_2 bubbles and Cl_2 on the electrodes surface can improve the rate of mass transfer even without use of a stirrer owing to stirring by turbulence in the solution.
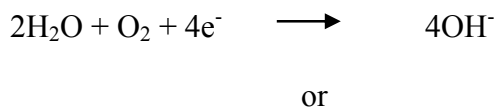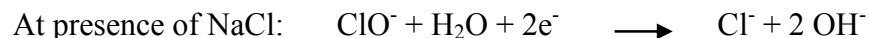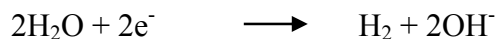
3.2.1. Kinetic investigations

The effects of the applied AC frequency, NaCl concentration, RB19 concentration, and solution stirring on the rate constant were investigated. The results presented in Table 3 show that NaCl has an enhancing effect on the rate constant because of the increased concentration of active oxidant species such as Cl_2/OCl^- in the solution[7]. The determination coefficient (R^2) of the plot for RB19 at two concentrations of 600 and 2000 mg/L was the highest, so the validity for the pseudo-first-order model is confirmed for these concentrations.

Frequent changes between acidification and alkalization can arise on the anode surface because of the cyclic nature of an AC signal[2, 22, 23]. The consecutive acidification and alkalization at the electrode surface prevents the oxide layer formation and activates the surface probably contributing to the increase in the self-corrosion rate of the anode. As AC frequency becomes higher, current reversal will be more rapid. Because of cyclic alternating of AC, the RB19 molecules can either gather or adsorb at the SS 304 surface. Consequently, both oxidation of adsorbed molecules and hydrogen producing can take place by the cyclic change[24].

## 3.3. Variation of solution pH, electrical conductivity, and ORP during EC process

The pH values of the experimental solution at the end of the EC treatment period are given in Fig. 3a. The initial pH of RB19 is pH of the RB19 solution without any pH adjustment. In all cases, a small increase in the pH values was obtained. It discloses that the rate of alkalization of the solutions increases. The rate of alkalization of the solutions near the SS 304 can play a major role in the electrodes weight loss by corrosion. The alkalization happens from changing cycles of AC, which electrochemically reduces water into OH^- [7, 25]. The ionization of RB19 occurs at pH=7.

$$2H_2O + O_2 + 4e^- \longrightarrow 4OH^-$$

or

11

$$2H_2O + 2e^- \longrightarrow H_2 + 2OH^-$$

At presence of NaCl: $\quad ClO^- + H_2O + 2e^- \longrightarrow Cl^- + 2\ OH^-$

The OH^- accumulates and results in pH change. Production of OH^- ions would increase the conductivity of the solution nearby the SS 304 electrodes. Another scenario is that under alkaline conditions the main anions is OH^-, which changes into $^\bullet OH$ radical by losing its electron to the electrode (anode) surface. The transfer of OH^- ions towards the anode is enhanced by AC frequency[26]. The increased production of these $^\bullet OH$ enhances the oxidation process of RB19.

Obtained result shows the rate of RB19 removal increases slightly with increasing EC treatment time and simultaneously increasing pH due to reduced loss of active chlorine via gaseous chlorine leaving the cell or the formation of chlorate. On the other hand, with increasing pH the oxidation potential of water decreases, leading to increase in undesirable water oxidation (at the anode). In the presence of chloride, oxidation of organic compounds is mediated by active chloro species [27, 28]. The main reactions at the electrodes are:
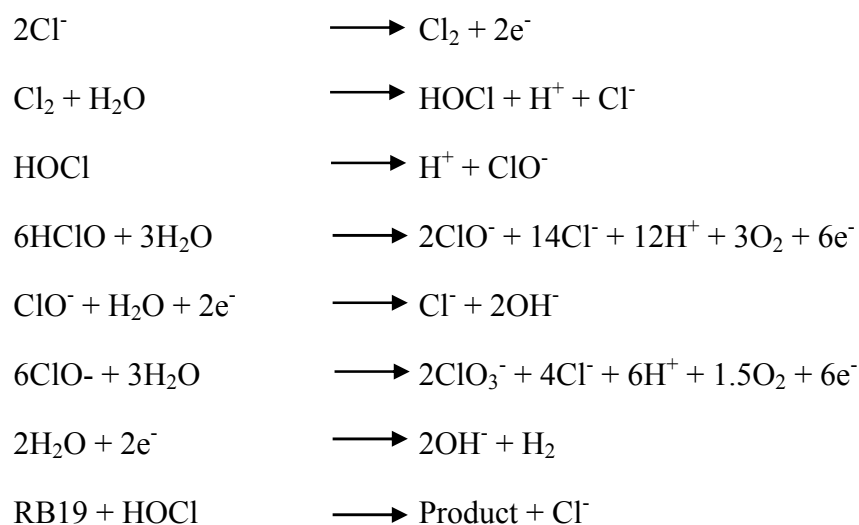
$$2Cl^- \longrightarrow Cl_2 + 2\ e^-$$
$$2H_2O + 2e^- \longrightarrow H_2 + 2OH^-$$
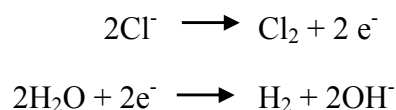
In the solution bulk, Cl_2 hydrolysis takes place as follows:

$$Cl_2 + H_2O \longrightarrow HOCl + H^+ + Cl^-$$

12

$$HOCl \longrightarrow H^+ + OCl^-$$

To study effects of wastewater conductivity on RB19 removal (Fig. 3b), experiments were performed using various amounts of NaCl to change the electrical conductivity of RB19 solution. With the NaCl concentration increasing, or equivalently, electrical conductivity (EC) (ms/cm) increasing, the ion concentration in RB19 solution increases, and the resistance between the electrodes reduces. The solution conductivity variation causes ion content variation. Ions that contribute to conductivity are H^+ and OH^- among others. As Fig. 3b shows, there was a slight increase in EC (ms/cm) during EC treatment, which indicates that NaCl salt is the main contributing agent to the conductivity of RB19 solution. However, EC with NaCl can lead to RB19 removal by following chloride reaction:

$$2Cl^- \longrightarrow Cl_2 + 2e^-$$

$$Cl_2 + H_2O \longrightarrow HOCl + H^+ + Cl^-$$

$$HOCl \longrightarrow H^+ + ClO^-$$

$$6HClO + 3H_2O \longrightarrow 2ClO^- + 14Cl^- + 12H^+ + 3O_2 + 6e^-$$

$$ClO^- + H_2O + 2e^- \longrightarrow Cl^- + 2OH^-$$

$$6ClO{-} + 3H_2O \longrightarrow 2ClO_3^- + 4Cl^- + 6H^+ + 1.5O_2 + 6e^-$$

$$2H_2O + 2e^- \longrightarrow 2OH^- + H_2$$

$$RB19 + HOCl \longrightarrow Product + Cl^-$$

Salt addition in RB19 solution improves the solution conductivity, but leads to increased amount of impurity in wastewater as well; although the electrical conductivity there is not effluent parameter limitations. The main ion released from

the SS 304 during EC process is iron, but the absolute value of the amount of released iron is very low. Iron is a biologically active element[29] and can influence the surrounding objects, i.e., the cells become subjected to electroporation. Furthermore, being an ion with changeable valence, the ferrous ion generates free radicals, which can essentially affect the results[29].

ORP of the RB19 solution under EC treatment steadily dropped to -374.9 ± -103.4 mV (Fig. 3c), indicating buildup of a reduced electrolyte condition. The reducing potential (negative ORP) is due to hydrogen gas production in the basic environment (pH$= 11.6 \pm 0.32$) [30].

3.4. Initial RB19 concentration

The initial RB19 concentration was varied in order to check its influence on the rate of RB19 removal. The rate of removal was the highest when the initial RB19 concentration was moderate (200–500 mg/L), while the removal rate decreased with increasing and decreasing initial RB19 concentration, as shown in Fig.3d. This may be explained by the fact that dye molecules with increasing concentration tends to associate with clusters of low diffusivity; this lowers the rate of dye diffusion to the electrode surface with a consequent decrease in the rate of dye oxidation[31, 32].

3.5. Energy Consumption

In any EC process, costs are incurred due to electrical energy demand, which affect

the operating costs. In the following section, electrical energy consumption was

calculated using different approaches.

3.5.1. EC based on power of function generator

The total energy consumption expresses the AC power (25 W) used to cause EC

reactions. Electrical energy consumption was calculated by using the following

equation:

$$EC\ (\text{kWhL}^{-1}) = \frac{P \times t}{V \times 60 \times log\frac{C_0}{C_t}} \qquad (3)$$

where P (kW) is the power, V is the volume (L) of treated RB19 solution, t is EC

treatment time (min), and C_0 and C_t are the concentrations of dye in (mg L^{-1} t) at

reaction time 0 and t, respectively.

3.5.2. EC for the removal of one kg of RB19

The energy consumption for the removal of one kg of RB19 is calculated by using

the following equation:

$$\text{Energy consumption(kWh m}^{-3}) = (\frac{[\frac{\frac{tVI}{Sv}}{1000}]}{\frac{\Delta RB19}{10^6}}) \qquad (4)$$

Here, t is the EC treatment time (h); V voltage in V, and I current in A; S_v the treated volume (L), and $\Delta RB19$ (g/L) the difference in RB19 concentration induced by the treatment. By using this equation, the energy consumption was calculated in kWh m^{-3}.

3.5.3. EC based on specific electrical consumption

Specific electrical energy consumption (E) per kg RB19 removal in EC process is a figure of merit, which is calculated using the following equation:

$$E(\text{kWh kg}^{-1} \text{ RB19}) = \frac{VIt}{S_v Y C_0} \tag{5}$$

where C_0 is the initial RB19 concentration (mg/L), t EC treatment time (min), V the voltage between electrodes (Vpp), and Y RB19 removal efficiency (%) [33] that is calculated by equation 2.

3.5.4. Estimation of energy consumption and operating cost

For EC process, the operating cost includes materials, mainly electrodes, and electrical energy costs. In this preliminary economic investigation, energy and electrode material costs were taken into account as major cost items in the calculation of the operating cost (Iranian Rial (IRR) and US$ per m^3 of RB19 solution) as below:

3.5.4.1. Operating cost based on required electrical energy and electrode material

$$\text{Operation cost}= aC_{energy} + bC_{electrode} \tag{6}$$

where C_{energy} and $C_{electrode}$ (kg m^{-3}) are consumption quantities for RB19 removal with SS 304 electrodes; they are obtained experimentally [34]. The electrical energy price, "a," and the electrode material price, "b," are given as follows according to the Iranian market in May 2015: "a"=US\$ 0.0129 per kW h, "b"= US\$ 3.344 per kg of SS 304. The cost for the electrical energy consumption was calculated by the following equation:

3.5.4.2. Electrical energy requirement

$$E_{energy} = \frac{VIt_{EC}}{S_v} \tag{7}$$

where V is the cell voltage (V), I the current (A), t_{EC} the EC process time (s), and S_v the RB19 solution volume (m^3) [35]. The electrode material cost was calculated using the Faraday's law in equation 8:

3.5.4.3. SS 304 electrodes requirement

$$C_{Electrode} = \frac{ItM_w}{zFS_v} \tag{8}$$

where I is the current (A), t the duration of EC (s), M_W the molecular mass of SS 304 (55.845 g mol^{-1}, the molar mass of Fe, was used in this study because the most abundant constituent of SS 304 is Fe), z the number of electron transferred

$(z = 2)$, F the Faraday's constant (96 487 C mol^{-1}), and V the volume (m^3) of RB19 solution.

Table 4 presents the results of electrical energy consumption estimated by all the methods described above. As can be seen, use of Na$_2$SO$_4$ electrolyte leads to the highest electrical energy consumption, and based on the RB19 removal efficiency and the operating cost, it is not recommended for EC dye removal process. In 2012, Iran reformed energy price and electrical policy, too[36]. According to Iran's Power Generation Transmission and Distribution Management Company (TAVANIR) reports, one kilowatt hour of electricity is sold for 430 Rials (about 0.017 cents) on average. Therefore, in comparison to the past, today electrical energy costs for dyes (RB19) removal has greater weight compared to the material cost for supplying SS 304 electrodes.

3.6. UV-visible absorption spectral changes

The alteration in the absorption spectrum (in both UV and visible range) for various time intervals during treatment of RB 19 through electro-oxidation is presented in Fig. 4. The peak observed in the visible is caused by blue color of chromophore, while the peak observed in the ultraviolet region is a result of the anthraquinone structure of RB19. The decrease of the visible peak during the electro-oxidation period might be due to the destruction of the quinine links by the attack of •OH radicals or other oxidants (Cl$_2$, OCl$^-$, and OH$^-$) produced during the

oxidation process. The absorbance reduction in the UV region (about 256 nm) is considered an evidence of chromophore degradation. As Fig. 4 presents, the peaks of treated RB19 at different treatment times are in accordance with those of the non-treated indicating that AC EC process can remove RB19 without producing intermediates[6].

3.7. Characterization of the sludge obtained from the EC reactor

A dark bluish precipitate formed at the bottom of the EC reactor as well as on the surface of RB19 solution at the end of EC process due to floatation of RB19 flocculated out of the solution by hydrogen bubbles. However, because of the cyclic polarity change at electrodes in AC mode, the sludge was raised around the electrodes, and its fouling phenomena were limited. The product was taken out of the solution and dried inside an oven for 3–4 h. It was then grinded to a fine powder and prepared for SEM and XRF analyses[37].

It was shown that the by-products formed during EC consisted of elements like Ni, Pb, Cr, and Cl, as well as metal oxides such as Fe_2O_3. The major constituent, loss on ignition (LOI), was measured to be 43.25% by weight of the EC sludge. LOI is a measure of the quantity of organic matter in a sample that can be combusted at 550°C. The loss in weight during combustion equates to the mass of organic matter in the sample. In other word, 43.25% of the EC sludge is organic matter or volatile solids content. It is thus related to the possible reduction of the sludge mass by

incineration. Volatile solids content is usually quoted as a percentage of the total solids residue. Solids content remaining after ignition (ash) is termed the fixed residue (FR), which defines the mass of inorganic matter in the sludge, and thus, the mass of solids that would remain for ultimate disposal after incineration.

The sludge can be divided into parts generally: 1) RB19-monomeric Fe and RB19-polymeric Fe that lead to RB19 precipitate; 2) RB19-polymeric Fe + $Fe_n(OH)_n$ that create the EC sludge.

The morphology of the by-products obtained from the EC reactor is shown in Fig. 5a. The sludge generated by SS 304 electrodes contains small particles that may be hydroxides, mainly Fe.

In order to gain more insight into the effects of AC, the morphology of the SS 304 electrode surface after several cycles of use was characterized by a camera as shown in Fig. 5b. It can be observed that the electrode surface is rough and disordered. Microstructure pores also formed around the nucleus of the active sites where electrode dissolution results in the production of Fe_2O_3. As a result, electrodes dissolved uniformly during the EC process[38].

SS 304 is non-magnetic (*i.e.*, has a low "permeability") and has excellent ductility, formability, and toughness, even at cryogenic temperatures. In sections with temperatures above 60°C, there is a risk of chloride-induced stress corrosion

cracking, often from the outside, in case the insulation material gets wet.

4. Conclusion

It can be concluded:

- Higher removal efficiencies of dye could be acquired when AMPL=8 Vpp and OFST=0.2 V were applied as the input voltage.

- Stirring of the solution led to a shorter required contact time.

- When used as a supporting electrolyte, NaCl provided with a higher RB19 removal efficiency than Na_2SO_4.

- ORP of the RB19 solution under EC treatment steadily dropped to -374.9 ± -103.4 mV, indicating buildup of a reduced electrolyte condition i.e., hydrogen gas production in the basic environment.

- UV-visible absorption spectral changes test showed the peaks of treated RB19 at different treatment times are in accordance with those of non-treated solution, demonstrating that AC EC treatment can remove RB19 without producing intermediates.

- Sludge study showed 43.25% of the EC sludge is organic matter or volatile solids content. It is thus related to the possible reduction of the sludge mass by incineration.

- Energy and electrode consumption was estimated by using different equations in our economic evaluation study. Results showed electrical

energy costs for this process are greater than the cost for supplying SS 304 electrodes. In general, energy and electrode consumption of the suggested system is much lower than that of DC mode systems.

References

1. R. Mao, X. Zhao, H. Lan, H. Liu and J. Qu, *Water Research*, 2015, **77**, 1-12.
2. M. Eyvaz, M. Kirlaroglu, T. S. Aktas and E. Yuksel, *Chemical engineering journal*, 2009, **153**, 16-22.
3. C. A. Martínez-Huitle and E. Brillas, *Applied Catalysis B: Environmental*, 2009, **87**, 105-145.
4. S. Singh, V. C. Srivastava and I. D. Mall, *RSC Advances*, 2013, **3**, 16426-16439.
5. A. Ahmad, S. H. Mohd-Setapar, C. S. Chuong, A. Khatoon, W. A. Wani, R. Kumar and M. Rafatullah, *RSC Advances*, 2015, **5**, 30801-30818.
6. M. Siddique, R. Farooq, Z. M. Khan, Z. Khan and S. Shaukat, *Ultrasonics sonochemistry*, 2011, **18**, 190-196.
7. J. B. Parsa, M. Rezaei and A. Soleymani, *Journal of hazardous materials*, 2009, **168**, 997-1003.
8. Y.-F. Wu and C.-H. Chen, *Journal of Alloys and Compounds*, 2013, **550**, 263-267.
9. E. Brillas and C. A. Martínez-Huitle, *Applied Catalysis B: Environmental*, 2015, **166–167**, 603-643.
10. A. Khatri, M. H. Peerzada, M. Mohsin and M. White, *Journal of Cleaner Production*, 2015, **87**, 50-57.
11. Y.-Z. Wang, A.-J. Wang, W.-Z. Liu, D.-Y. Kong, W.-B. Tan and C. Liu, *Bioresource Technology*, 2013, **146**, 740-743.
12. A. Pirkarami, M. E. Olya and S. Raeis Farshid, *Water Resources and Industry*, 2014, **5**, 9-20.
13. M. R. Samarghandy, E. Hoseinzadeh, M. Taghavi and A. Rahmani, *BioResources*, 2011, **6**, 4840-4855.
14. E. Hoseinzadeh, A. Reza Rahmanie, G. Asgari, G. McKay and A. Reza Dehghanian, *Journal of Scientific and Industrial Research*, 2012, **71**, 682.
15. K. Malachova, Z. Rybkova, H. Sezimova, J. Cerven and C. Novotny, *Water Research*, 2013, **47**, 7143-7148.
16. X. Quan, X. Zhang and H. Xu, *Water Research*, 2015, **78**, 74-83.
17. E. Hoseinzadeh, M.-R. Samarghandi, G. McKay, N. Rahimi and J. Jafari, *Desalination and Water Treatment*, 2014, **52**, 4999-5006.
18. L. Li and Y. Liu, *Journal of Hazardous Materials*, 2009, **161**, 1010-1016.
19. D. Rajkumar and J. G. Kim, *Journal of hazardous materials*, 2006, **136**, 203-212.
20. B. Z. Can, R. Boncukcuoglu, A. E. Yilmaz and B. A. Fil, *Journal of Environmental Health Science and Engineering*, 2014, **12**, 95.
21. B. Khaled, B. Wided, H. Béchir, E. Elimame, L. Mouna and T. Zied, *Arabian Journal of Chemistry*, 2014, DOI: http://dx.doi.org/10.1016/j.arabjc.2014.12.012.
22. M. Y. A. Mollah, R. Schennach, J. R. Parga and D. L. Cocke, *Journal of hazardous materials*, 2001, **84**, 29-41.
23. X. Mao, S. Hong, H. Zhu, H. Lin, L. Wei and F. Gan, *Journal of Wuhan University of Technology-Mater. Sci. Ed.*, 2008, **23**, 239-241.
24. R. Juchniewicz, J. Jankowski and K. Darowicki, *Materials Science and Technology*, 2000.

25. I. Arslan-Alaton, I. Kabdaşlı, D. Hanbaba and E. Kuybu, *Journal of hazardous Materials*, 2008, **150**, 166-173.
26. K. Forthun, 2013.
27. D. A. C. Coledam, J. M. Aquino, R. C. Rocha-Filho, N. Bocchi and S. R. Biaggio, *QuÃ-mica Nova*, 2014, **37**, 1312-1317.
28. R. Misra, N. N. Neti, D. D. Dionysiou, M. Tandekar and G. S. Kanade, *RSC Advances*, 2015, **5**, 10799-10808.
29. T. Tomov and I. Tsoneva, *Bioelectrochemistry*, 2000, **51**, 207-209.
30. A. Ciblak, X. Mao, I. Padilla, D. Vesper, I. Alshawabkeh and A. N. Alshawabkeh, *Journal of Environmental Science and Health, Part A*, 2012, **47**, 718-726.
31. E. El-Ashtoukhy, N. Amin and M. Abdel-Aziz, *Int. J. Electrochem. Sci*, 2012, **7**, 11137-11148.
32. E. Nossol, A. B. S. Nossol, A. J. G. Zarbin and A. M. Bond, *RSC Advances*, 2013, **3**, 5393-5400.
33. C. K. Araújo, G. R. Oliveira, N. S. Fernandes, C. L. Zanta, S. S. L. Castro, D. R. da Silva and C. A. Martínez-Huitle, *Environmental Science and Pollution Research*, 2014, **21**, 9777-9784.
34. D. Ghosh, C. Medhi and M. Purkait, *Chemosphere*, 2008, **73**, 1393-1400.
35. S. Vasudevan, B. S. Kannan, J. Lakshmi, S. Mohanraj and G. Sozhan, *Journal of Chemical Technology and Biotechnology*, 2011, **86**, 428-436.
36. K. Amirnekooei, M. Ardehali and A. Sadri, *Energy*, 2012, **46**, 374-385.
37. S. Vasudevan, J. Lakshmi and G. Sozhan, *Journal of hazardous materials*, 2011, **192**, 26-34.
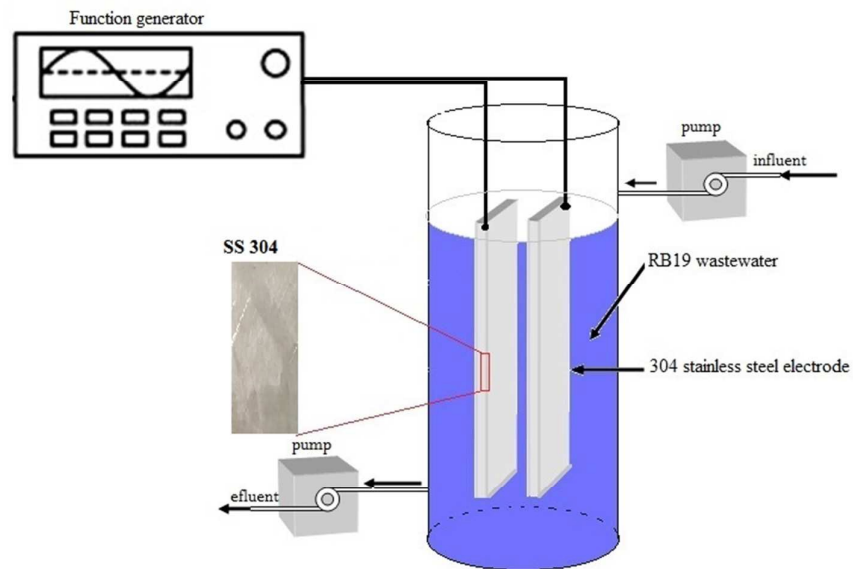38. S. Vasudevan and J. Lakshmi, *Water Science & Technology*, 2012, **65**, 353-360.

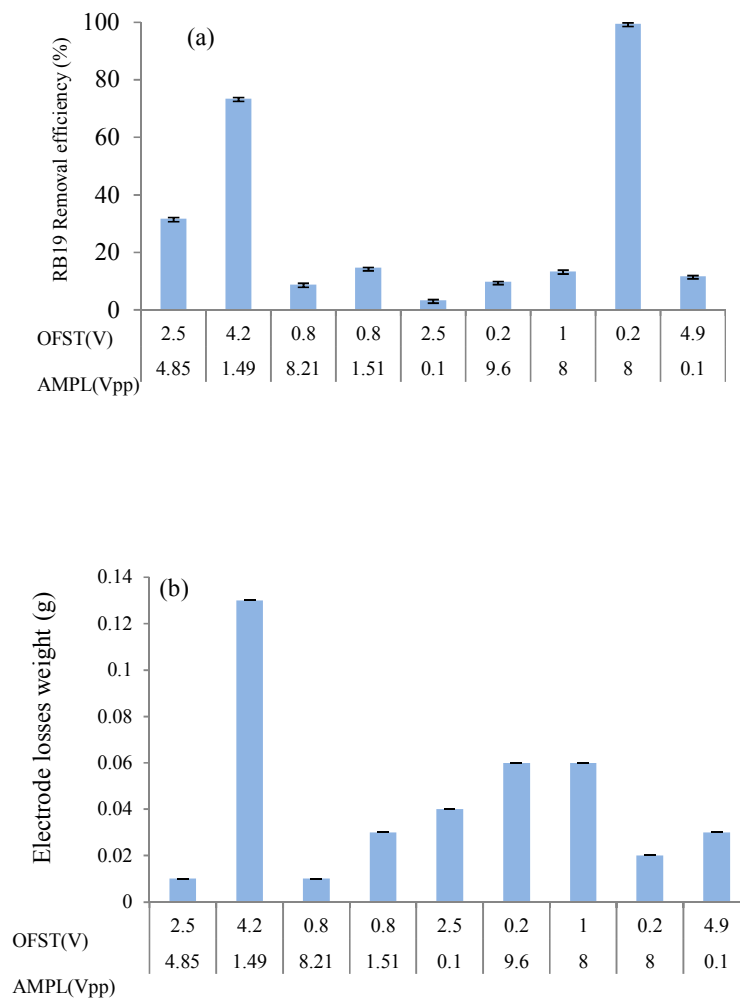Fig. 1. Electrochemical reactor used in the present study

Fig. 2. Effects of applied AMPL and OFST: a) Effect of applied AMPL and OFST pairs on RB19 removal efficiency in EC process; b) Effect of applied AMPL and OFST pairs on electrode weight loss in EC process.
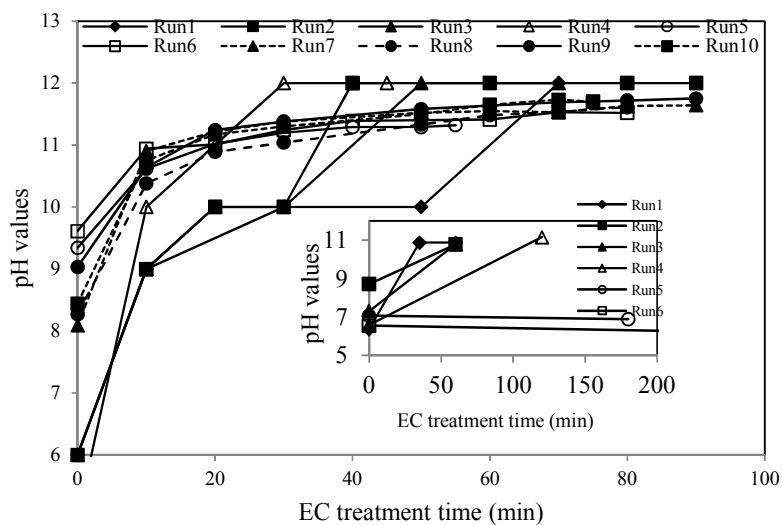
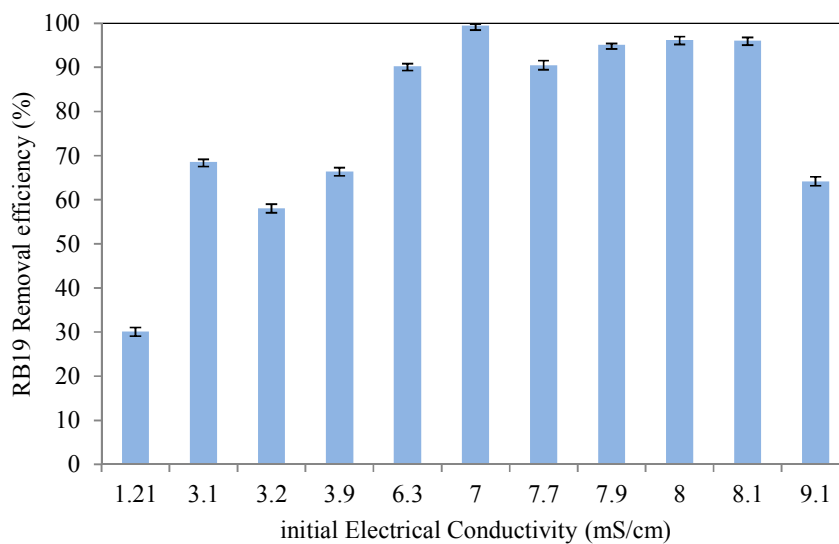Fig. 3a. Variation of pH value during EC process; small graph is related to the stirring mode

Fig. 3b. Variation of electrical conductivity value during EC process; small graph is related to the stirring
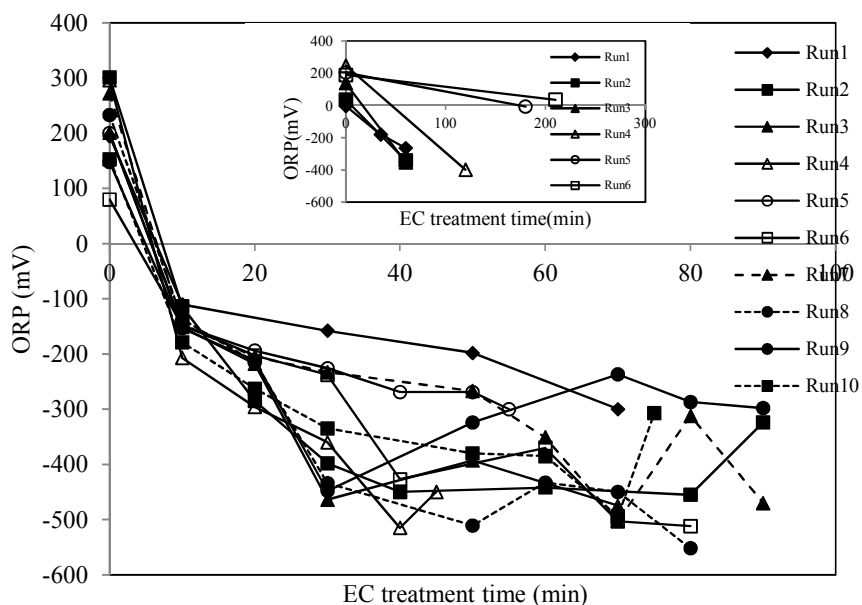
mode

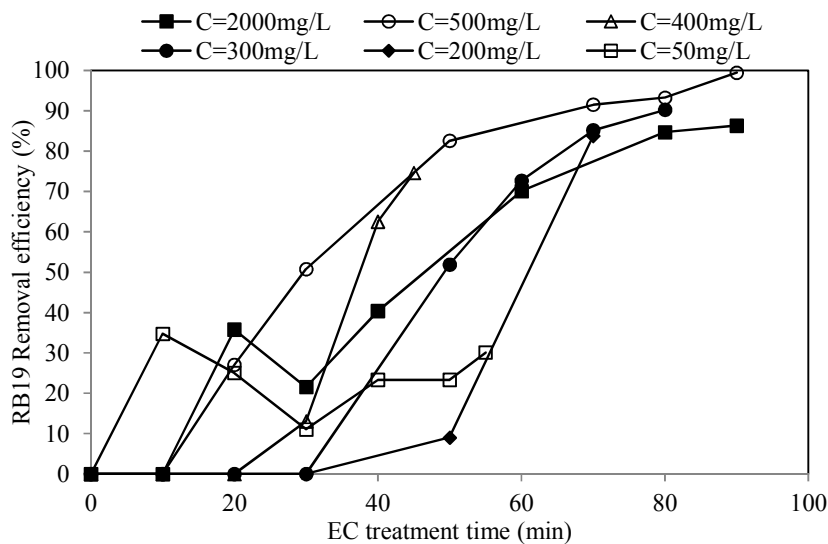Fig. 3c. Variation of ORP value during EC process; small graph is related to the stirring

mode

Fig. 3d. Effect of initial RB19 concentration on the removal efficiency
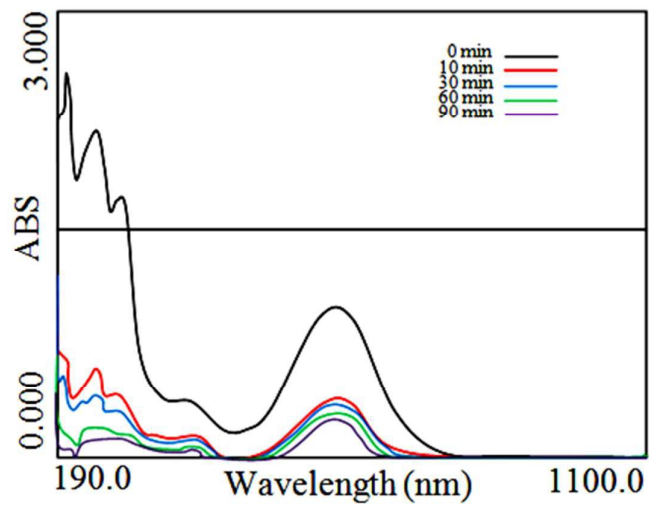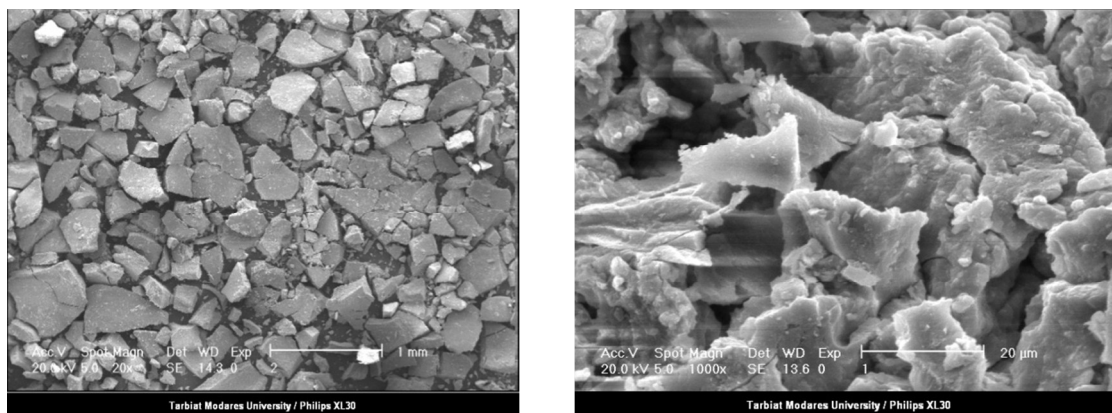
Fig. 4. UV-visible absorption spectral changes by electrochemical process for various treatment time

composition	LOI	Na$_2$O	MgO	Al$_2$O$_3$	SiO$_2$	P$_2$O$_5$	Ni
W%	43.257	2.862	0.324	0.401	2.22	1.526	2.318
composition	SO$_3$	Cl	CaO	Cr	MnO	Fe$_2$O$_3$	Pb
W%	3.827	6.402	0.254	5.255	0.469	30.82	0.065

Fig. 5a. SEM and XRF results from the sludge produced after EC treatment of RB19 with SS 304 electrodes
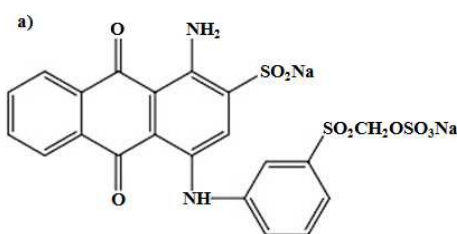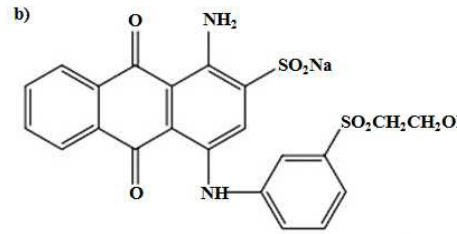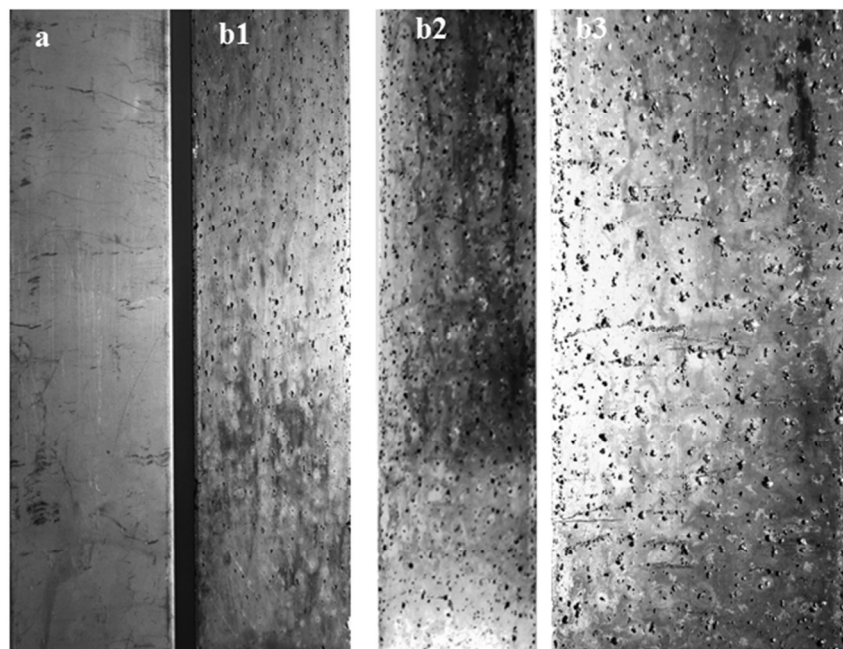

Fig. 5b. Photo of SS 304 surface: a) SS 304 without EC; b1, b2, and b3) SS 304 in EC process at various magnifications.

Table 1. Chemical composition and physical and mechanical properties of stainless steel

Chemical composition		echanical properties		physical properties	
elemen t	**%**	Tensile Strength (MPa)	520-720	Density	8.00 g/cm^3
C	0-0.07	Compression Strength (MPa)	210	Melting Point	1450°C
Mn	0-2.0			Modulus of Elasticity	193 GPa
Si	0-1	Proof Stress 0.2% (MPa)	210	Electrical Resistivity	0.072×10^{-6} Ù.m
P	0-0.05				
S	0-0.02	Elongation A5 (%)	45 Min	Thermal Conductivity	16.2 W/m.°K
Cr	17.5-19.5				
Ni	8-10.5	Hardness Rockwell B	92	Thermal Expansion	17.2×10^{-6} °K
Fe	Balance				

Table 2: main characteristics of RB19 dye

Chemical name	Remazol Brilliant Blue R	
C.l. Generic name	C.l.Reactive Blue 19	
Chemical class	Anthraquinone	
Chemical name	2-(3-(4-Amino-9,10-dihydro-3-sulpho-9,10-dioxoanthracen-4-yl) aminobenzenesulphonyl)vinyl) disodiumsulphate	
Formula	$C_{22}H_{10}O_{11}N_2S_3Na_2$	
λ_{max} (nm)	594	
Molecular weight (g/mol)	626.5	
Biodegrability (%)	<10	
Toxicity to fish, CL50 (mg/L)	500-1000	
Chemical structure		a) un-hydrolyzed, b) hydrolyzed